Intramolecular Excimer Formation and Photoinduced Electron-Transfer Process in Bis-1,8-Naphthalimide Dyads Depending on the Linker Length

ARTICLE *in* THE JOURNAL OF PHYSICAL CHEMISTRY A · AUGUST 2008

Impact Factor: 2.69 · DOI: 10.1021/jp801983b · Source: PubMed

4 AUTHORS, INCLUDING:

Dae Won Cho
Korea University
106 PUBLICATIONS **1,401** CITATIONS

SEE PROFILE

THE JOURNAL OF PHYSICAL CHEMISTRY A

Article

Intramolecular Excimer Formation and Photoinduced Electron-Transfer Process in Bis-1,8-Naphthalimide Dyads Depending on the Linker Length

Dae Won Cho, Mamoru Fujitsuka, Akira Sugimoto, and Tetsuro Majima

J. Phys. Chem. A, **2008**, 112 (31), 7208-7213 • DOI: 10.1021/jp801983b • Publication Date (Web): 12 July 2008

Intramolecular Excimer Formation and Photoinduced Electron-Transfer Process in Bis-1,8-Naphthalimide Dyads Depending on the Linker Length

Dae Won Cho,[†,‡] Mamoru Fujitsuka,[†] Akira Sugimoto,[†] and Tetsuro Majima*[,†]

The Institute of Scientific and Industrial Research (SANKEN), Osaka University, Mihogaoka 8-1, Ibaraki, Osaka 567-0047, Japan, and Department of Chemistry, Chosun University, Gwangju 501-759, Korea

Received: March 6, 2008; Revised Manuscript Received: April 28, 2008

The photophysical properties of bis-1,8-naphthalimide (NI−L−NI) dyads with different linkers ($L = -C_3H_6-$, $-C_4H_8-$, $-C_6H_{12}-$, $-C_8H_{16}-$, and $-C_9H_{18}-$) as well as the reference NI derivative ($NI-C_7H_{15}$) were investigated in CH_3CN and H_2O/CH_3CN (v/v = 1:9). The normal fluorescence peak of ^{1}NI*−L−NI was observed at 379 nm together with a broad emission at longer wavelength both in aprotic CH_3CN and in H_2O/CH_3CN, which is assigned to an excimer, ^{1}(NI−L−NI)*. The excimer emission maximum was blue-shifted with increasing length of the linker. The photoinduced electron-transfer process of NI−L−NI was also investigated in both solvents by using nanosecond-laser flash photolysis. The T_1-T_n absorption band for ^{3}NI*−L−NI was observed around 470 nm in both solvents. In H_2O/CH_3CN, NI−L−NI is solvated with H_2O in the ground state to exist as solvated NI−L−NI. In the excited triplet state, the NI radical anion ($NI^{\bullet-}$) was generated via the intramolecular quenching of ^{3}NI*−L−NI by another NI moiety. The solvated $NI^{\bullet-}$−L−NI may undergo the proton abstraction process to give $NI(H)^{\bullet}$−L−NI, which can be confirmed by the transient absorption band at 410 nm. This band was not observed in pure aprotic CH_3CN.

Introduction

Polycyclic aromatic hydrocarbons including 1,8-naphthalimide (NI) are known to form an excimer that is stable in the excited state but dissociable in the ground state. These can be confirmed by markedly red-sifted structureless emission, which has no corresponding absorption spectrum.[1] An intramolecular excimer, generated from two aromatic hydrocarbon linked together by a polymethylene chain, reveals the molecular dynamics of the chain and can be used as sensors for conformational changes in molecular assemblies,[2] polymers[3] and biosystems.[4] Barros et al.[5] reported the intramolecular excimer emissions around 480 nm of bis-NI dyads connected by short methylene chains. We reported the formation of intermolecular excimer of NI in nonpolar solvents.[6] These reports imply that NI can interact strongly with each other.

On the other hand, NI derivatives have been used in many studies of the photoinduced electron transfer (PET) involving NI and various donor molecules because these compounds have excellent electron-acceptor properties.[7] There are two kinds of PET processes. One is an intermolecular PET process between electron donor (D) and acceptor (A) molecules, leading to the formation of various radical ion pairs as well as subsequent chemical reactions. The other is an intramolecular PET process for D−A molecules bridged by various linkers (L), namely, dyad and triad systems, leading to the charge-separated state ($D^{\bullet+}-L-A^{\bullet-}$), which might lead to synthetically useful chemical reactions.[8] There are several reports that an excited NI is a good electron acceptor and ground-state NI can act as an electron donor.[9–11] We have conjectured that the intermolecular PET process between NI and NI could occur easily in a protic polar solvent. However, the PET between NI and NI has not yet been systematically studied. Hence, the objectives of this study are to understand the linker effect in the intramolecular excimer formation and the role of protic polar solvent in the intramolecular PET process.

In this work, we prepared various bis-1,8-naphthalimides (NI−L−NI) dyads having different linkers ($L = -C_3H_6-$ (C3), $-C_4H_8-$ (C4), $-C_6H_{12}-$ (C6), $-C_8H_{16}-$ (C8), and $-C_9H_{18}-$ (C9)), and the reference NI (NI−C7) having $-C_7H_{15}$ on the nitrogen atom, as shown in Scheme 1. We have carried out the time-resolved emission measurement and nanosecond-laser flash photolysis studies of NI−L−NI and NI−L to elucidate the photodynamic properties.

Experimental Section

Materials. Syntheses of NI−L−NI and reference NI−C7 molecules were carried out as follows.

***N*-Heptyl-1,8-naphthalimide (NI−C7).** The detail of synthesis of NI−C7 has been described earlier.[6] Bis-NI compounds were prepared by two kinds of reaction methods: the reaction of metalated naphthalimide (NI) with dihaloalkane (method A), or the reaction of 1,8-naphthalic anhydride (NA) with diaminoalkane (method B). ^{1}H NMR spectra were measured at room temperature using a JEOL JMN LA-400.

1,8-*N*-Propyldinaphthalimide (NI−C3−NI). The mixture of NA (800 mg), 1,3-diaminopropane (150 mg), and *p*-xylene (70 mL) was refluxed for 6 h according to method B. After removal of solvent, the residue was purified by chromatography with dichloromethane−ethyl acetate gave colorless solid. Yield: 300 mg (25%), mp > 300 °C. ^{1}H NMR ($CDCl_3$): 2.25 (m, 2H), 4.37 (t, 4H), 7.73 (m, 4H), 8.20 (m, 4H), 8.57 (m, 4H). FAB-MS *m*/*z* calcd for $C_{27}H_{19}N_2O_4$ $[M + H]^+$ 435.1345, found 435.69.

1,8-*N*-Butyldinaphthalimide (NI−C4−NI). To a suspension of sodium hydride (50%, 200 mg) in dimethylformamide (DMF) (10 mL) was added a solution of NI (800 mg) in DMF (15 mL), and the mixture was heated at 70 °C for 1 h under stirring.

* To whom correspondence should be addressed. E-mail: majima@saken.osaka-u.ac.jp.
† Osaka University.
‡ Chosun University.

10.1021/jp801983b CCC: $40.75
Published on Web 07/12/2008

SCHEME 1: Structure of Bis-1,8-naphthalimides and Reference Molecule

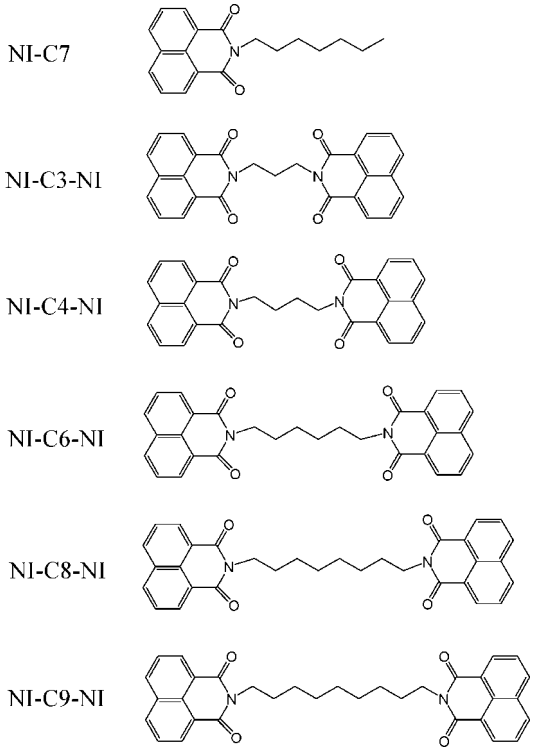

After the addition of 1,4-dibromobutane (0.24 mL) and DMF (10 mL), the reaction mixture was stirred at 80 °C for 5 h and stirred for overnight at room temperature by method A. The solid deposited was collected by filtration, chromatographed over silica gel with chloroform, and recrystallized from dichloroethane. Yield: 510 mg (57%), mp > 300 °C. ^{1}H NMR ($CDCl_3$): 1.90 (m, 4H), 4.27 (br. s, 4H), 7.74 (m, 4H), 8.20 (m, 4H), and 8.58 (m, 4H). FAB-MS *m*/*z* calcd for $C_{28}H_{21}N_2O_4$ $[M + H]^+$ 449.1501, found 449.61.

1,8-*N*-Hexyldinaphthalimide (NI−C6−NI). This compound was prepared by a similar method to that described in literature.[12] To a suspension of NI (800 mg) in ethanol (2 mL) was added a solution of potassium hydroxide (265 mg) in ethanol (5 mL). To this mixture was added 1,6-dibromohexane (500 mg) and DMF (3 mL), and then the mixture was refluxed for 1 h according to method A. The solid deposited was filtered off and the filtrate was evaporated to dryness. The residue was purified by chromatography with dichloromethane−methanol and repeated crystallization from dichloroethane. mp: 259.5−261 °C. ^{1}H NMR ($CDCl_3$): 1.52 (m, 4H overlap with that of H_2O), 1.76 (m, 4H), 4.19 (t, 4H), 7.74 (m, 4H), 8.21 (m, 4H), and 8.58 (m, 4H). FAB-MS *m*/*z* calcd for $C_{30}H_{25}N_2O_4$ $[M + H]^+$ 477.1814, found 477.73.

1,8-*N*-Octyldinaphthalimide (NI−C8−NI). This compound was prepared from 1,8-diiodooctane (732 mg), NI (800 mg), and sodium hydride (50%: 200 mg) in DMF as a solvent by method A. Purification by means of chromatography with dichloromethane to give pure compound. Yield: 480 mg (48%), mp 210−211 °C. ^{1}H NMR ($CDCl_3$): 1.39 (m, 8H), 1.73 (m, 4H), 4.17 (t, 4H), 7.74 (m, 4H), 8.20 (m, 4H), and 8.60 (m, 4H). FAB-MS *m*/*z* calcd for $C_{32}H_{29}N_2O_4$ $[M + H]^+$ 505.2127, found 505.80.

1,8-*N*-Dodecyldinaphthalimide (NI−C9−NI). This compound was prepared from 1,9-diaminononane (791 mg) and NA (1.98 g) in toluene (120 mL) by method B. Purification by means of chromatography with dichloromethane to give pure compound. Yield: 100 mg (10%), mp 175.5−177 °C. ^{1}H NMR ($CDCl_3$): 1.37 (m, 10H), 1.71 (m, 4H), 4.17 (t, 4H), 7.74 (m, 4H), 8.19 (m, 4H), and 8.59 (m, 4H). FAB-MS *m*/*z* calcd for $C_{33}H_{31}N_2O_4$ $[M + H]^+$ 519.2284, found 519.80.

General Techniques. Time-resolved fluorescence spectra were measured by the single photon counting method using a streakscope (Hamamatsu Photonics, C4334-01) equipped with a polychromator (Acton Research, SpectraPro150). Ultrashort laser pulse was generated with a Ti:sapphire laser (Spectra-Physics, Tsunami 3941-M1BB, fwhm 100 fs) pumped with a diode-pumped solid-state laser (Spectra-Physics, Millennia VIIIs). For excitation of the sample, the output of the Ti:sapphire laser was converted to THG (300 nm) with a harmonic generator (Spectra-Physics, GWU-23FL). The instrument response function was also determined by measuring the scattered laser light to analyze a temporal profile. This method gives a time resolution of about 50 ps after the deconvolution procedure. The temporal emission profiles were well fitted into a single- or double-exponential function. The residuals were less than 1.1 for each system.

Steady-state UV−vis absorption spectra were recorded with a UV−vis spectrophotometer (Shimadzu, UV-3100) at room temperature. Fluorescence spectra were measured using a Hitachi 850 fluorophotometer. Fluorescence quantum yields were measured using anthracene in toluene as a standard with a known ϕ_f of 0.30.[13] The excimer-emission quantum yields in longer wavelength were cross-checked using perylene in toluene as a standard with a known ϕ_f of 0.75.[14] The emission quantum yields were determined after the deconvolution using the fluorescence spectrum of reference NI−C7 with an excitation wavelength of 320 nm.

Transient absorption measurements were carried out by employing the technique of ns-laser flash photolysis. The third harmonic generation (THG, 355 nm) of Q-switched Nd:YAG laser (Surelite, pulse width of 5 ns fwhm) was used to excite the samples. Pulse energy was ca. 18 mJ pulse^{-1}. A Xenon flash lamp (Osram, XBO-450) was focused into the sample solution as the probe light for the transient absorption measurement. Temporal profiles were measured with a monochromator (Nikon, G250) equipped with a photomultiplier (Hamamatsu Photonics, R928) and a digital oscilloscope (Tektronix, TDS-580D). A Hamamatsu Photonics multichannel analyzer (C5967) system also was used for measurement of the transient absorption spectra. The whole system was controlled with a personal computer by means of a GP-IB interface. Reported signals were average of 50 events. All solutions were argon-saturated unless otherwise indicated.

Results and Discussion

Steady-State Absorption and Emission Spectra. The absorption and fluorescence spectra of NI−L−NI and NI−C7 in CH_3CN are shown in Figure 1. A salient feature of the absorption spectra of NI−L−NI is resemblance to that of reference NI−C7; this implies that there is no strong interaction between two NI moieties in the ground state. On the other hand, the absorption maxima of NI−L−NI and NI−C7 were slightly shifted to long wavelength in protic H_2O/CH_3CN (v/v = 1:9) (Table S1 in Supporting Information). This red shift can be understood by the hydrogen bonding effect of water solvent.[15]

The fluorescence spectra of NI−L−NI dyads in CH_3CN shows two bands in the short (SW, 379 nm) and long wavelengths (LW, 425−491 nm), as shown in Figure 1 (those in H_2O/CH_3CN are shown in Figure S1 in Supporting Information). Table 1 lists the emission maxima of NI derivatives

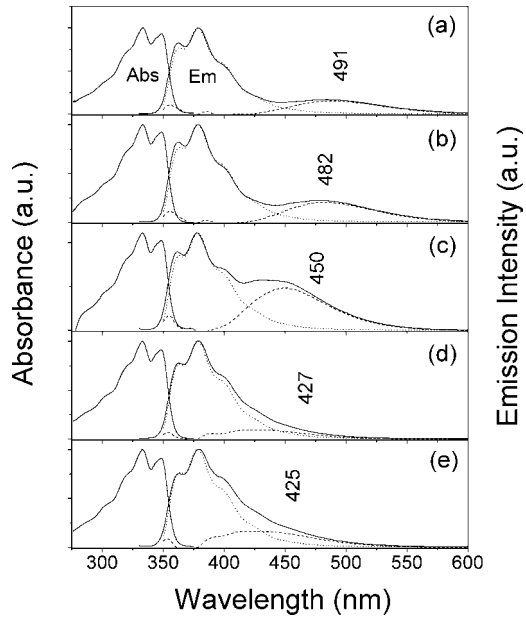

Figure 1. Steady-state absorption and fluorescence spectra of NI−L−NI (solid lines) and NI−C7 (dotted lines) in CH_3CN: (a) NI−C3−NI, (b) NI−C4−NI, (c) NI−C6−NI, (d) NI−C8−NI, and (e) NI−C9−NI. The excimer emission spectra of NI−L−NI (dashed lines) are estimated though the subtraction of fluorescence spectrum of NI−C7 from those of NI−L−NI. The excitation wavelength is 330 nm.

TABLE 1: Emission Maxima of NI Derivatives in CH_3CN and H_2O/CH_3CN[a]

	in CH_3CN		in H_2O/CH_3CN	
NI derivatives	monomer	excimer	monomer	excimer
NI−C7	378		384	
NI−C3−NI	379	491 (500)	385	499 (504)
NI−C4−NI	379	482 (489)	385	488 (499)
NI−C6−NI	379	450 (464)	385	457 (463)
NI−C8−NI	379	427 (438)	385	434 (445)
NI−C9−NI	379	425 (436)	385	443 (451)

[a] Parenthetical values for the excimer are determined from the time-resolved emission spectra.

measured in both solvents. SW emission of NI−L−NI shows a clear vibronic structure and the identical emission maxima at 379 nm. SW bands are the mirror image of the absorption spectra. SW emission is generated from ^{1}NI*−L−NI in the singlet excited state. SW fluorescence quantum yields (ϕ_f^{SW}) of NI−L−NI in CH_3CN were found to be 0.032−0.058, as listed in Table 2. On the other hand, the ϕ_f^{SW} in H_2O/CH_3CN are larger than those in CH_3CN.

The solvent dependence of ϕ_f^{SW} of NI−L−NI can be rationalized in terms of two closely located upper excited triplet (n,π^*, T_2) and excited singlet (π,π^*, S_1) states. A close proximity of the two states can promote the intersystem crossing process in a nonpolar solvent.[15] On the other hand, the ϕ_f increases in polar solvents. The protic polar solvent forms the hydrogen bond with the excited molecules. It also affects on the energy gap between T_2 and S_1 states. This is clearly pronounced in H_2O/CH_3CN for NI−L−NI, which has fluorescence quantum yields larger than 0.13, whereas their corresponding values are less than 0.058 even in highly polar solvent such as CH_3CN as listed in Table 2.

The emission spectra of NI−L−NI showed an extra emission band at long wavelength. In the case of NI−C3−NI, LW emission maximum is observed at 491 nm. Because the

TABLE 2: Fluorescence Lifetimes (τ_f) and Fluorescence Quantum Yields (Φ_f) of NI−L−NI in CH_3CN and H_2O/CH_3CN[a]

	in CH_3CN				in H_2O/CH_3CN			
	monomer		excimer		monomer		excimer	
compound	τ_f (ns)	Φ_f^{SW}	τ_f (ns)	Φ_f^{LW}	τ_f (ns)	Φ_f^{SW}	τ_f (ns)	Φ_f^{LW}
NI−C7	0.14	0.021			0.61	0.14		
NI−C3−NI	0.24	0.059	26	0.0080	0.78	0.16	29	0.018
NI−C4−NI	0.19	0.042	28	0.0090	0.61	0.16	31	0.025
NI−C6−NI	0.17	0.037	23	0.018	0.49	0.15	28	0.059
NI−C8−NI	0.18	0.033	10	0.0060	0.52	0.15	12	0.026
NI−C9−NI	0.17	0.032	15	0.0070	0.49	0.14	15	0.026

[a] The Φ_f values for the excimer of NI−L−NI were determined after the deconvolution. All quantum yields were measured within 5% error. The temporal emission profiles were well fitted into single-exponential function. The residuals were less than 1.1.

reference NI−C7 does not show LW emission, LW emission of NI−L−NI can be assigned to the intramolecular excimer ^{1}(NI−L−NI)* originated from the interaction between excited NI and ground-state NI moieties. We can reasonably exclude the intermolecular excimer formation, because the solubility of NI−L−NI is very low in CH_3CN as well as H_2O/CH_3CN. The optical density of saturated NI−L−NI solutions in a cell with 1.0 cm of optical path is less than 0.37 at 330 nm. This means that the concentration of NI−L−NI solution is less than 2.9×10^{-5} M, which was determined by the previously reported ϵ value (12600 M^{-1} cm^{-1} at 330 nm) in cyclohexane.[15] Moreover, the ratio of relative intensity between SW and LW emissions did not change with reducing concentration of ~10 times from saturated solutions. This indicates that the excimer emission independents on the concentration of NI−L−NI. Barros et al.[4] also reported the excimer emissions for ^{1}(NI−C3−NI)* and ^{1}(NI−C4−NI)* around 480 nm.

The intramolecular excimer formation of NI−L−NI is favorable even in low concentrated CH_3CN solution, because NI moieties are connected by the flexible linkers. Intramolecular excimer formation by association interaction between excited NI and NI moiety can be expected to be equally possible both in polar and in nonpolar solvents. The excimer emissions of NI−L−NI were also observed in H_2O/CH_3CN (Figure S1 of Supporting Information), which were not observed in reference NI−C7 in the same solvent. The excimer emission maxima of NI−L−NI in H_2O/CH_3CN are red-shifted than in CH_3CN, because of the hydrogen bonding.

It is noteworthy that the excimer emission maximum of NI−L−NI shifted to a short wavelength with increasing length of linkers. When two NI moieties are in contact, the excitation energy of any one moiety can be delocalized; in a simplified picture this can be thought of as the relaxation of electronic excitation by forming a dimer. This interaction is the basis of the stability of excimer, as shown in Scheme 2. It is significant in a highly concentrated solution, the large arrays of molecules in polymer or crystal. However, the excimer formation on NI−L−NI dyads is more efficient, because two NI moieties are intrinsically close.

The energy of excimer emission (ΔE in Scheme 2) is affected by the followings: (1) the distance between two NI moieties, and (2) the angles between the polarization axes for the transition considered.[16,17] NI−L−NI derivatives can have a lot of conformers, because the energy barrier of conformational change of C−C single bond is very low, and NI moieties are connected by flexible linkers. Although details about conformational structures of NI−L−NI are not known, the average distances

SCHEME 2: Interaction of HOMO and LUMO Orbitals of Two Molecules NI* and NI[a]

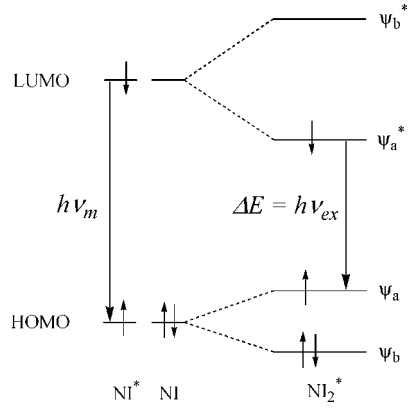

[a] $h\nu_m$ is the fluorescence of monomer NI* and $h\nu_{ex}$ is the excimer emission.

between NI and NI moieties could be related with the carbon-numbers of linker.

The emission spectrum of NI−C9−NI shows the excimer emission maximum at shorter wavelength than others. This blue shift of excimer emission of NI−L−NI derivatives could be explained in terms of a longer distance between two NI moieties than others. In the case of longer linkers such as NI−C9−NI, the excimer emission showed the low intensity and much overlap with a normal emission. Although the overall emission feature of NI−C9−NI is similar to the normal emission of NI−C7, it is important that there is the intramolecular long-range interaction.

The quantum yields of excimer emission showed low values compared with those of the SW emission (Table 2). Although it can be expected that the $\pi-\pi$ interaction of NI−C3−NI favors the face-to-face excimer, the highest excimer emission yield (ϕ_f^{LW}) among NI−L−NI derivatives was observed in NI−C6−NI (Table 2). The excimer peaks of NI−L−NI in nonpolar 1,4-dioxane (the solubility is very poor in other nonpolar solvents such as *n*-hexane) showed the blue shifts about 6 nm compared with those in CH_3CN. This indicates that NI−L−NI has the partially charge-transferred character. The charge-transfer type excimer formation does not require the exact face-to-face conformation. Thus, charge-transfer character decreases the ϕ_f^{LW} value when the linker is shorter. On the other hand, a larger linker also decreases the ϕ_f^{LW} value. These two factors are reason for the highest yield of excimer for NI−C6−NI.

Time-Resolved Emission Spectra. Figure 2 is the time-resolved fluorescence spectra of NI−L−NI in CH_3CN obtained by the femtosecond pulse excitation. In H_2O/CH_3CN, the time-resolved emission spectra of NI−L−NI are shown in Figure S2 of Supporting Information. At 30 ps after the excitation, the time-resolved emission spectra of NI−L−NI show the emission around 380 nm, which corresponds to the steady-state SW emission. The decays of SW emission of NI−L−NI are faster than 240 ps. The decay time constants of NI−L−NI are shown in Table 2. The SW emission around 380 nm disappeared in the spectra at 1.5 ns after excitation. Consequently, the excimer emission around 430−500 nm appeared. First of all, it is noteworthy that the time-resolved excimer emission of NI−L−NI shifts to a short wavelength according to the increase of the length of linkers. The excimer emission maxima appeared at slightly longer wavelength compared with those from steady-state emission spectra (Table 1). The excimer emission lifetimes of NI−L−NI were measured to be over 10 ns.

The rise component from the time-resolved excimer emission spectra of NI−L−NI could not be resolved, because the excimer

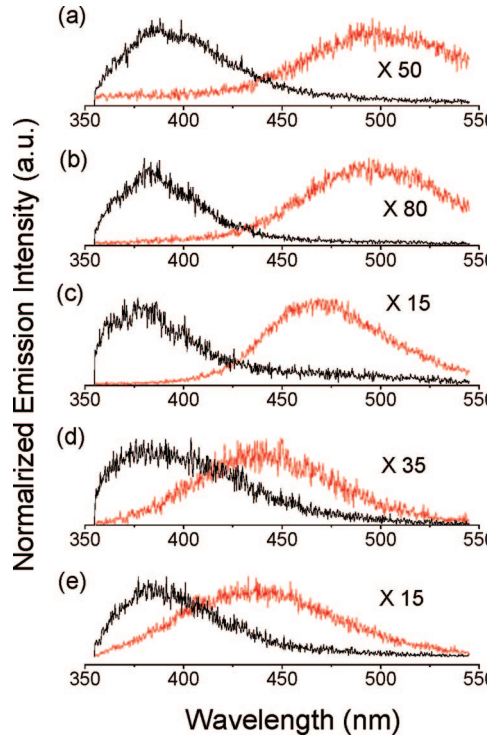

Figure 2. Time-resolved emission spectra of NI−L−NI molecules in CH_3CN: (a) NI−C3−NI, (b) NI−C4−NI, (c) NI−C6−NI, (d) NI−C8−NI, and (e) NI−C9−NI. The shorter wavelength and excimer spectra were measured with the delay time of 30 ps (black) and 1.5 ns (red), respectively, after the laser pulse excitation.

emission is much overlapped with the SW emission. However, it could be suggested that the time constant for excimer formation relates to the decay time constant of the SW emission.

Transient Absorption Spectra. The transient absorption spectra of NI−L−NI were obtained during the nanosecond-laser flash photolysis measurement with 355 nm excitation. The transient absorption spectra of NI−C3−NI (2.9×10^{-5} M) were measured in CH_3CN and H_2O/CH_3CN, as shown in Figure 3. The transient absorption spectrum of NI−C3−NI in CH_3CN shows a characteristic band around 470 nm, which is identical to the T_1-T_n absorption of NI in the triplet excited state (^{3}NI*) reported in our earlier work.[13] The transient absorption of NI−C3−NI in CH_3CN decayed with first-order kinetics of the lifetime of 3.1 μs at both wavelengths (410 and 470 nm), as shown in inset of Figure 3a. In CH_3CN, other NI−L−NI derivatives also showed only the T_1-T_n absorption band at 470 nm without any other transient absorption bands. The decay time constants for NI−L−NI derivatives monitored at 470 nm are 3.1−13 μs (Table 3).

In protic H_2O/CH_3CN, the T_1-T_n absorption of NI−C3−NI was also observed at 470 nm, as shown in Figure 3b. In addition to this band, a weak transient absorption band was observed at around 410 nm. The bands at 470 and 410 nm showed the different kinetic traces, as shown in inset of Figure 3b. The T_1-T_n absorption at 470 nm decayed with 4.1 μs of lifetime. On the other hand, the transient absorption band at 410 nm showed a slow growth (~4.1 μs, comparable to the decay of triplet state), and then a very slow decay of >20 μs. The transient absorptions of other NI−L−NI also showed two bands around 410 and 470 nm in H_2O/CH_3CN. The decay times at 470 nm were 4.1−11.8 μs for NI−L−NI derivatives. The slow growth of transient absorptions at 410 nm occurred concomitantly with the decay of the T_1-T_n absorption at 470 nm. This implies that a long-lived transient species should be produced

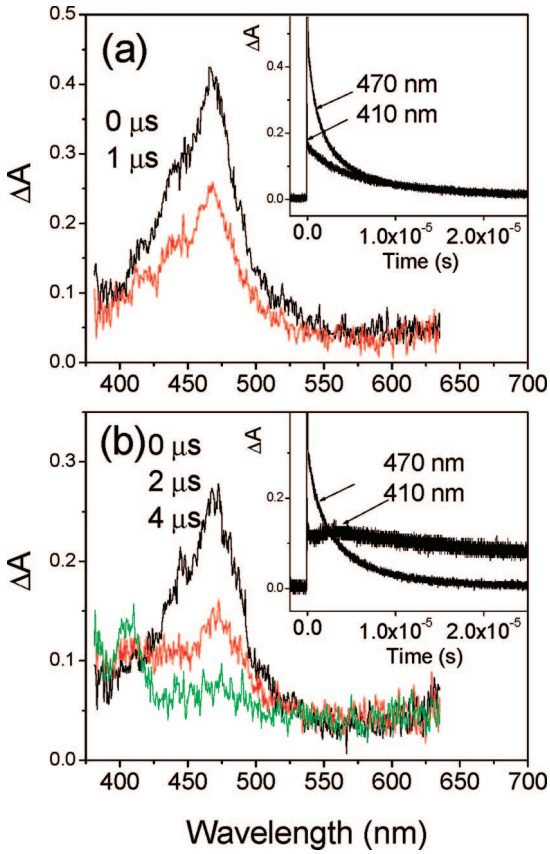

Figure 3. Transient absorption spectra of NI−C3−NI (2.9×10^{-5} M) in (a) CH_3CN and (b) H_2O/CH_3CN (v/v = 1:9) observed during the nanosecond-laser flash photolysis (excitation wavelength = 355 nm). The inset shows kinetic traces of ΔA at 410 and 470 nm: (a) decay times are 2.8 μs monitored at 410 and 470 nm, respectively; (b) decay times are 20 and 2.8 μs monitored at 410 and 470 nm, respectively.

TABLE 3: Triplet-State Decay Time Constants of ^{3}NI* (τ_T) and NI(H)$^\bullet$ (τ_K) in CH_3CN and H_2O/CH_3CN (v/v = 1:9)

compound	in CH_3CN τ_T (μs)	in H_2O/CH_3CN τ_T (μs)	in H_2O/CH_3CN τ_K (μs)
NI−C7	2.7	3.5	38
NI−C3−NI	3.9	5.3	18
NI−C4−NI	8.2	10.1	25
NI−C6−NI	10.4	10.6	40
NI−C8−NI	7.0	7.3	80
NI−C9−NI	4.7	6.0	65

after the formation of ^{3}NI* which is the precursor of the new transient species giving an absorption band at 410 nm. The transient absorptions at 410 nm of NI−L−NI decayed with very long lifetimes (ca. >20 μs).

The ^{3}NI*−L−NI should act as the main precursor of NI$^{\bullet-}$−L−NI as described by following equations. NI$^{\bullet-}$−L−NI could be generated through the *intramolecular* reaction. On the basis of the previous suggestion by some reports,[9–11] which described a competitive and efficient deactivation pathway of ^{3}NI*, the mechanistic pathways could be summarized as shown in eq 2, which might lead to the quenching of ^{3}NI* moiety by another NI moiety of NI−L−NI. Recently, the formation and decay times of monomeric NI$^{\bullet-}$ showed strong dependence on the concentration of NI. This implies that NI$^{\bullet-}$ could be primarily generated via the quenching of ^{3}NI* by NI at the diffusion control rate as shown in eq 3, but not efficient in case of NI−L−NI because of low concentration.

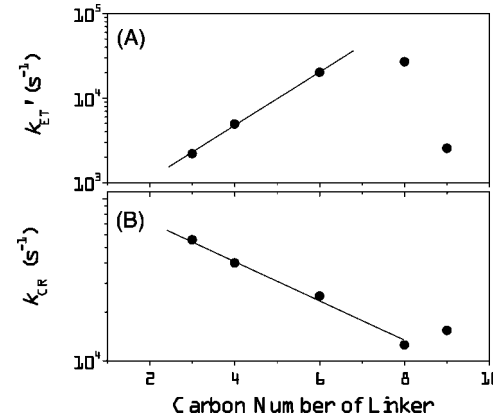

Figure 4. (A) Logarithmic plot of the electron-transfer rate constant (k_{ET}') vs the carbon number of linker. (B) Logarithmic plot of the charge recombination rate constant (k_{CR}) vs the carbon number of linker.

$$\mathrm{NI{-}L{-}NI} \xrightarrow{h\nu} {}^1\mathrm{NI^*{-}L{-}NI} \xrightarrow{\mathrm{ISC}} {}^3\mathrm{NI^*{-}L{-}NI} \quad (1)$$

$${}^3\mathrm{NI^*{-}L{-}NI} \xrightarrow{\mathrm{PET}} \mathrm{NI^{-\bullet}{-}L{-}NI^{+\bullet}} \quad (2)$$

$${}^3\mathrm{NI^*{-}L{-}NI} + \mathrm{NI{-}L{-}NI} \xrightarrow{\mathrm{PET}} \mathrm{NI^{-\bullet}{-}L{-}NI} + \mathrm{NI^{+\bullet}{-}L{-}NI} \quad (3)$$

In the case of reference ^{3}NI*−C7, the decay rate constant in CH_3CN is 1.33 times higher than that in H_2O/CH_3CN. The decay rate constants of ^{3}NI*−L−NI in CH_3CN are also higher than those in H_2O/CH_3CN. On the other hand, the ratio of decay rate-constants ^{3}NI*−L−NI in H_2O/CH_3CN and CH_3CN is increased. We assumed that this increasing is due to the electron-transfer process in H_2O/CH_3CN. The rate constant of electron transfer corrected by solvent effect (k_{ET}') could be calculated using the following eq 4,

$$k'_{ET} = \left\{ (k_{T,NI-L-NI})_W - (k_{T,NI-L-NI})_A \times \frac{(k_{T,NI-C7})_W}{(k_{T,NI-C7})_A} \right\} \quad (4)$$

where $(k_T)_A$ and $(k_T)_W$ are the decay constants of ^{3}NI* in CH_3CN and H_2O/CH_3CN, respectively. The linker-length dependence of k_{ET}' for N−L−NI is shown in Figure 4A. The k_{ET}' for NI−C3−NI to NI−C6−NI rises exponentially with increasing carbon number of linkers. The k_{ET}' for NI−C8−NI to NI−C9−NI does not lie along the straight line established by NI−C3−NI to NI−C6−NI. The highest rate constant of NI−C6−NI indicates that the PET occurs fast. This result consists of the high quantum yield for the intramolecular excimer formation of NI−C6−NI. The rate constants for charge recombination (k_{CR}) in NI−L−NI are obtained from the decay rate of transient absorption changes at 410 nm. Charge recombination within NI−C3−NI to NI−C8−NI is exponential (Figure 4B). The rate constant for charge recombination in NI−C9−NI did not follow. The photophysical and kinetical parameters are changed in NI−C6−NI to NI−C8−NI, in fact, it seems due to the increase of inhomogeneity as well as the degree of freedom with increasing linker length.

It is well-known that NI$^{\bullet-}$ has a transient absorption band at around 420 nm. In spite of the similarity for the transient absorption bands between NI$^{\bullet-}$ and NI(H)$^\bullet$, the transient absorption band observed at 410 nm in H_2O/CH_3CN could

SCHEME 3: Structure of ketyl radical of NI

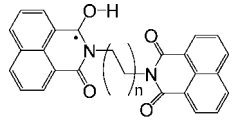

NI(H)•-L-NI

not be attributed to $NI^{\bullet -}$ because this band could not be observed in aprotic CH_3CN but be observed in protic H_2O/CH_3CN. It indicates that $NI^{\bullet -}$ may undergo the fast protonation process to give NI(H)•, as shown in Scheme 3 and eq 5, which shows the transient absorption band at 410 nm.[18]

$$H_2O\cdot\cdot\cdot NI^{-\bullet}-L-NI \rightarrow NIH^{\bullet}-L-NI + OH^{-} \qquad (5)$$

Because NI(H)• is not charged species, the transient absorption band of 410 nm has a long lifetime related to a charge recombination process.

Conclusion

This study demonstrates the long-range interaction for the intramolecular excimer formation of NI−L−NI. The eximer emissions significantly shift to shorter wavelength according to the length of linkers between the two NI moieties. This study clearly shows that NI can easily interact with other NI moiety, which resulted to intramolecular excimer formation. Furthermore, NI−L−NI showed the PET process in H_2O/CH_3CN, which can be formed mainly by the intramolecular interaction between $^3NI^*$ and NI moieties.

Acknowledgment. This work has been partly supported by a Grant-in-Aid for Scientific Research (Project 17105005, 19350069, Priority Area (477) and others) from the Ministry of Education, Culture, Sports, Science and Technology (MEXT) of Japanese Government.

Supporting Information Available: Table of absorption maxima. Figures of absorption, fluorescence, and emission spectra. This material is available free of charge via the Internet at http://pubs.acs.org.

References and Notes

(1) Birks, J. B. *Photophysics of Aromatic Molecules*; Wiley Interscience: New York, 1970; Chapter 7.

(2) (a) Turro, N. J.; Aikawa, M.; Yekta, A. *J. Am. Chem. Soc.* **1979**, *101*, 772. (b) Desvergne, J. P.; Fages, F.; Bouas.Laurent, H.; Matsau, P. *Pure Appl. Chem.* **1992**, *64*, 1231.

(3) Yoshizawa, H.; Ashikaga, K.; Yamamoto, M. *Polymer* **1989**, *30*, 534.

(4) Prigogine, I.; Rice, S. A. *Advances in Chemical Physics: Electron Transfer - from Isolated Molecules to Biomolecules*; John Wiley & Sons Inc: New York, 2007; Part 1, Vol. 106.

(5) Barros, T. C.; Filho, P. B.; Toscano, V. G.; Politi, M. J. *J. Photochem. Photobiol. A: Chem.* **1995**, *89*, 141.

(6) Cho, D. W.; Fujitsuka, M.; Choi, K. H.; Park, M. J.; Yoon, U. C.; Majima, T. *J. Phys. Chem. B* **2006**, *110*, 4576.

(7) Rogers, J. E.; Weiss, S. J.; Kelly, L. A. *J. Am. Chem. Soc.* **2000**, *122*, 427.

(8) (a) Yoon, U. C.; Mariano, P. S. *Acc. Chem. Res.* **1992**, *25*, 233. (b) Yoon., U. C.; Mariano, P. S. *Acc. Chem. Res.* **2001**, *34*, 523.

(9) Aveline, B. M.; Matsugo, S.; Redmond, R. W. *J. Am. Chem. Soc.* **1997**, *119*, 11785.

(10) Li, H. Q.; Jiang, Z. Q.; Wang, X.; Pan, Y.; Wang, F.; Yu, S. O. *Res. Chem. Intermed.* **2004**, *30*, 369.

(11) Kelly, L. A. *I-APS Newsletter* **2001**, *24*, 14.

(12) Mattocks, A. M.; Hutchison, O. S. *J. Am. Chem. Soc.* **1948**, *70*, 3474.

(13) Cho, D. W.; Fujitsuka, M.; Sugimoto, A.; Yoon, U. C.; Mariano, P. S.; Majima, T. *J. Phys. Chem. B* **2006**, *110*, 11062.

(14) Murov, S. L.; Carmichael, I.; Hug, G. L. *Handbook of Photochemistry*, 2nd ed.; Marcel Dekker: New York, 1993.

(15) Wintgens, V.; Valet, P.; Kossanyi, J.; Biczok, L.; Demeter, A.; Berces, T. *J. Chem. Soc., Faraday Trans.* **1994**, *90*, 411.

(16) Becker, R. S. *Theory and Interpretation of Fluorescence and Phosphorescence*; Wiley & Sons, Inc.: New York, 1969.

(17) Suppan, P. *Chemistry and Light*; The Royal society of Chemistry: Cambridge, U.K., 1994.

(18) Demeter, A.; Biczók, L.; Bérces, T.; Wintgens, V.; Valat, P.; Kossanyl, J. *J. Phys. Chem.* **1993**, *97*, 3217.

JP801983B